City, University of London Institutional Repository

This is the published version of the paper.

This version of the publication may differ from the final published version.

Rotational capacity of exposed base plate connections with various configurations of anchor rod sleeves

Mohamed A. Shaheen [a],[*], Konstantinos Daniel Tsavdaridis [b], Felipe Piana Vendramell Ferreira [c], Lee S. Cunningham [d]

[a] *School of Architecture, Building and Civil Engineering, Loughborough University, Loughborough, UK*
[b] *Department of Engineering, School of Science & Technology, City, University of London, Northampton Square, EC1V 0HB London, UK*
[c] *Faculty of Civil Engineering – Campus Santa Mônica, Uberlândia, Federal University of Uberlândia, Minas Gerais, Brazil*
[d] *School of Mechanical, Aerospace and Civil Engineering, The University of Manchester, Manchester, UK*

A B S T R A C T

This paper presents a new approach that can enhance the rotational capacity of exposed base plate connections without degrading the initial stiffness or strength of the standard configuration. By inserting a steel sleeve with a designated geometry between the base plate and the anchor rod washer, the load path between the end plate and the rod can be interrupted, promoting a more ductile response. Exposed base plate connections with various sleeve geometries are numerically investigated using a validated FE model to demonstrate the concept of the proposed method. It was concluded that the proposed sleeve system substantially enhances the rotational capacity of the exposed column bases. An elastic response consistent with standard base plate connections is maintained indicating that the proposed system is compatible with existing codified elastic design approaches without modification.

1. Introduction

Exposed column bases are extensively used in low-to-medium rise steel structures. The ductility of a steel frame can be controlled by the strength and rotational capacity of the column bases. Under extreme loading conditions such as seismic action, plastic hinges at the ground floor column can be accommodated either in the lower region of the column (i.e., strong base approach) or in the base plate connection (i.e., weak base approach). The strong base approach is common in engineering practice [1] since the components of the base connection are presumed to be brittle with limited ductile response compared with the steel section. This brittle response was evidenced by premature failure of base plate connections during the 1994 Northridge Earthquake in the United States [2]. Designing the base plate connection to be stronger than the column requires a complex and expensive layout (e.g. using stiffeners and multiple anchor rods) and/or excessive amount of material (e.g. using thick end plates). The weak base approach, in which the plastic deformation concentrates within the base connection, is permitted by both BS EN 1998 [3] and AISC 341 [4]. Japanese design practice allows the plastic hinge to be in the column base connection if

the anchor rod has guaranteed and sufficient deformation capacity, otherwise the plastic hinge would be in the column itself and the base plate connection must be designed to remain in the elastic stage [5,6]. Despite the adoption of the weak base approach in prevalent design codes, it is not popular in practice since the ductility provided by the base plate connection is not guaranteed as evidenced in previous failures.

Experimental tests conducted on standard exposed base plate connections have provided insights into the behaviour of such connections concluding that the rotational capacity under cyclic loading ranges between 0.03 rad to 0.05 rad depending on the failure mode and the connection detailing [7–10]. Falborski et al. [11] carried out a parametric study to examine the strength and deformation capacity of the base plate connection on the probability of collapse of steel moment frames. It was concluded that structural performance of the frames improved with the rotational capacity of the base plate. The base plate should have sufficient rotational capacity such as 0.05 rad (rad) to achieve satisfactory structural performance for the steel frames examined by [11]. The study considered limited moment frame layouts; thus, the 0.05 rad rotation capacity cannot be generalised as significantly

* Corresponding author.
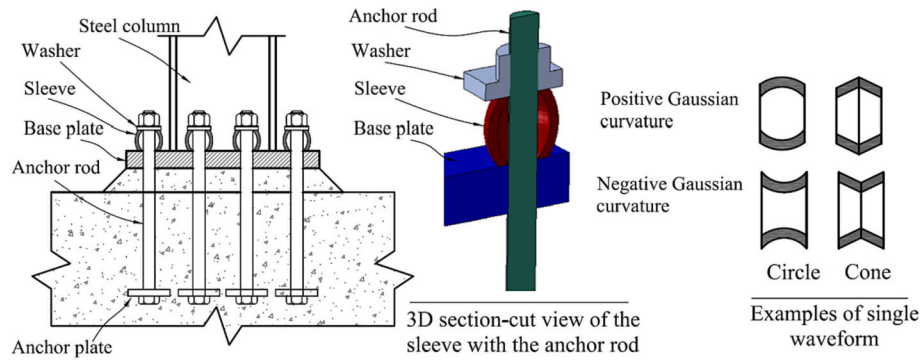*E-mail address:* m.shaheen@lboro.ac.uk (M.A. Shaheen).

Fig. 1. Proposed base plate connection with sleeves.

Fig. 2. Possible failure modes corresponding to sleeve capacity.

higher rotation may be needed for other layouts of frames. Elkady et al. [12] carried out a series of experimental tests on slender steel columns under lateral and axial force concluding that column sections may have limited ductility due to local buckling which is then followed by lateral instability at a rotation ranging between 0.02 and 0.1 rad. The base plate connection should have similar rotation range considering that the rotation of the column and the base plate connection are similar due to the frame kinematics. Despite the fact that some base plate connections studied in the existing literature have been shown to achieve this range of rotational capacity [8,13], compact cross-sections can undergo larger rotation beyond the reported values form the aforementioned study. Further, the columns invistgated by Elkady et al. exhibited a small rotation due to the 2nd order effect (P-Δ effect) which is applicable for moment resisting frames. Columns in a braced frame, for example, are less affected by the P-Δ effect and the ductility of the structure is significantly controlled by the rotational capacity of the base plate. The column rotational capacity reported by Elkady et al. [12] also implies that adopting the strong base approach forces the plastic rotation into the column itself which could be the least ductile element in the load path resulting in a brittle behaviour. Overall, the rotational demand of the base plate connection is yet to be investigated, however it is generally accepted that the higher the rotational capacity the better the overall structural performance. Further, field observations from the 2010 Maule earthquake in Chile showed that building with ductile base connections provided excellent seismic performance [14].

Limited research in the existing literature has focused on enhancing the rotational capacity of exposed base plate connections as opposed to that for beam-column connections. Several researchers proposed the ductile anchor concept in which long anchor rods with a designated stretch length are used to provide large component elongation and subsequently higher rotational capacity of base connections [5,6,8,13,15]. Various tests were carried out on individual anchor rods under tension [16] and combined shear and tension [17] to investigate the effect of stretch length on the deformation capacity, concluding that

a stretch length of more than four times the rod diameter can improve the ductility of the connection compared to a conventional anchor bolt. Test results of base plate connections designed in accordance with the ductile anchor rod concept with various stretch lengths have demonstrated a rotation capacity up to 0.12 rad [8,13]. However, long anchor rods may result in higher flexible responses of the base plate connection as the stiffness is inversely proportional to the anchor length. Zareian et al. [18] examined the effect of the base flexibility on the seismic response of steel frames and concluded that the base fixity alters the plastic mechanism, significantly reduces the rotational capacity of the steel frame and increases the member forces. Thus, increasing the rotation capacity of the base connection can have negative consequences on the overall frame ductility and performance when the initial stiffness is degraded. Further, the ductile anchor rod approach cannot be easily implemented for retrofitting of existing structures as this requires partial demolition of the foundation. The present study proposes a novel method to enhance the rotational capacity of exposed base plate connections while maintaining the initial stiffness and capacity of the standard configuration. The proposed method can be used to enhance the rotational capacity of an existing exposed base plate connection with low cost.

2. System description

Fig. 1 illustrates the column base connection with the proposed sleeve system. The sleeve is defined by length, thickness and wall curvature and is inserted between the base plate and the washer of the anchor rod. The sleeve can be described as a shell of revolution (see definition in [19]) or more simply as a barrel shape that resists the applied load by a combination of membrane and bending stresses, with the latter becoming more significant as the ratio between the sleeve thickness and the radius of curvature is increased [15]. A curvature in the sleeve wall is introduced to promote failure by bending rather than instantaneous buckling of the sleeve wall which can promote a dynamic
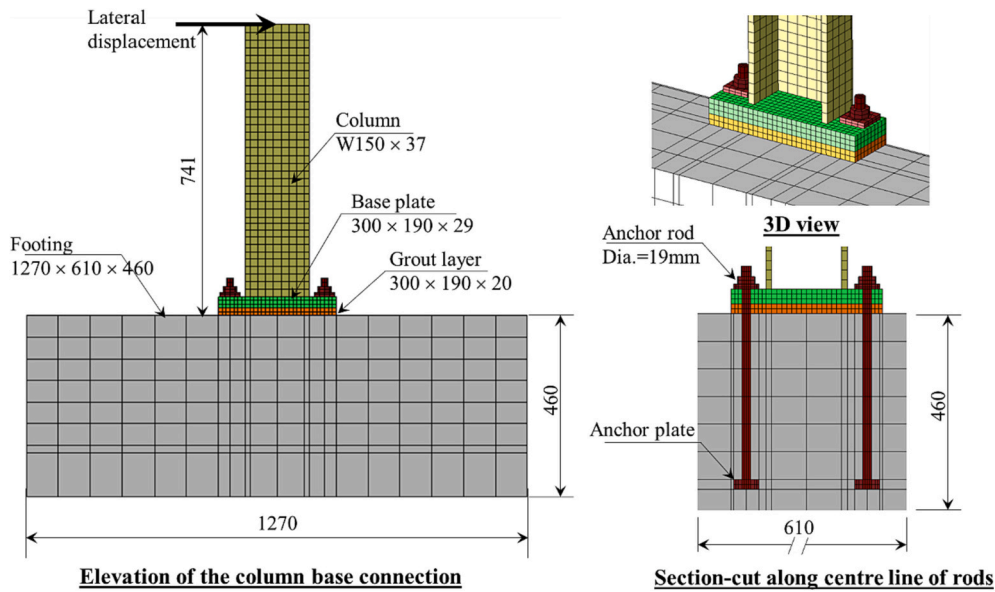
Fig. 3. FE model of the column base connection (all dimensions are in mm).
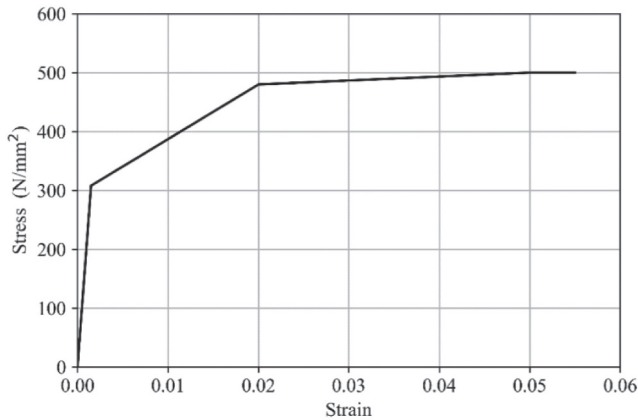

Fig. 4. Stress-strain response of the anchor rod material.

effect. This curvature is defined based on the amplitude at the mid-length of the sleeve and the corresponding geometrical equation of the waveform. In theory, there are countless waveform configurations that can define the sleeve configuration, however, the optimal waveform is the one that can achieve the best structural performance and the lowest fabrication cost. Positive and negative Gaussian curvature are applicable

for the same waveform, however, the latter requires a washer with very specific dimensions as the outer radius of the sleeve can be larger than the washer radius after introducing the amplitude. Furthermore, the bearing between the sleeve with negative Gaussian curvature and the washer can result in high internal forces in the washer which may require a non-standard thick washer. Therefore, only the sleeve with positive Gaussian curvature is considered in this study.

To provide increased ductility, bending deformation must develop in the sleeve before the failure of any connection components. To achieve this, the ultimate capacity of the sleeve should be lower than the force in the anchor rod at failure. For instance, if anchor rod failure is the controlling failure mode, the sleeve capacity should be designed such that it fails and crushes between the washer and the base plate before the anchor rod failure. There are three distinct combinations of connection behaviour, depending upon the sleeve amplitude as shown in Fig. 2 including: (i) when a small amplitude value is used (Fig. 2(a)), the sleeve capacity would be higher than the bolt capacity resulting in the sleeve undergoing limited elastic deformation causing the bolts to fail without achieving any significant enhancements to rotational capacity, (ii) increasing the amplitude value such that the sleeve capacity is slightly higher than the bolt capacity results in limited plastic deformation before bolt failure (Fig. 2(b)), and (iii) exploiting the optimal or plastic amplitude (PA), the sleeves exhibit significant plastic deformation eventually crushing between the end plate and the washer before bolt
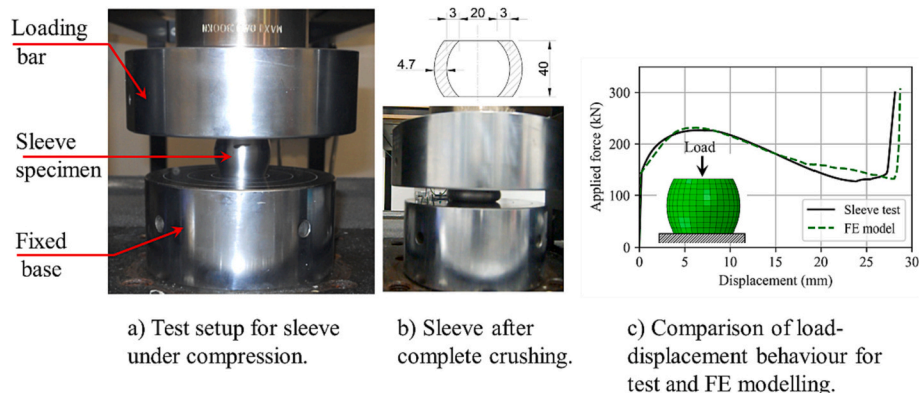

a) Test setup for sleeve under compression.

b) Sleeve after complete crushing.

c) Comparison of load-displacement behaviour for test and FE modelling.

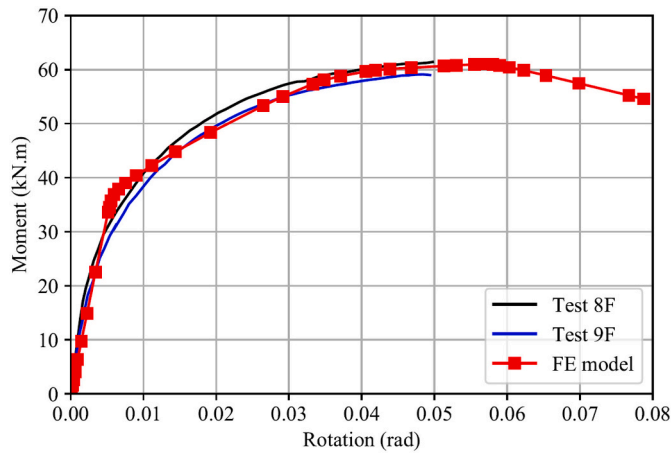**Fig. 5.** FE validation of single sleeve under compression.

3

Fig. 6. Comparison of experimental and numerical results for moment vs. rotation.

failure as shown in Fig. 2(c). The sleeve acts as a structural fuse under extreme loading conditions concentrating the damage in the sleeve part and protecting the other structural components, which can be then easily replaced after the damaging event. Furthermore, the sleeve can be considered as a good energy dissipation device due to the plastic deformation that can be developed under the applied load. The proposed device can also be used for retrofitting existing exposed base plate connections that possess brittle performance with minimal cost. The sleeve can be inserted between the base plate and the washer without the need for breaking-out the foundation or the connection. However, if

the existing anchor rod does not have sufficient length to accommodate the sleeve between the washer and the base plate, it can be extended by using a coupling nut or welding [1]. If welding is used to extend the anchor rod, special care should be taken to assure that the anchor rod grades being welded are made from weldable steel and will not be detrimentally affected by the weld process. Detailed guidance on extending an existing anchor rod can be found in AISC Steel Design Guide 1 [1]. In the case of damage under extreme loading, the proposed system could reduce repair costs, as the damage would be localised to the sleeve rather than the column or the other connection's components.

Shaheen et al. [20–23] conducted numerical and analytical investigations to prove the concept of the proposed sleeve method for the case of beam end-plate connections. The previous analyses concluded that the proposed system substantially enhances the rotational capacity of such connections, which is imperative for progressive collapse and earthquake resistance, without degrading either the initial stiffness of the standard configuration or the load-bearing capacity.

The aim of the present study is twofold. Firstly, to prove the concept of using the sleeve device to increase the rotational capacity of the exposed base plate connection without degrading its elastic behaviour nor its capacity. Second, to conduct a parametric study of base plate connections with the proposed sleeve device and various configurations in order to assess the effect of the sleeve geometric parameters. It should be noted that the forthcoming investigation is confined to the specific case of monotonic loading, hence the conclusions drawn cannot be directly applied to other loading scenarios such as cyclic loading without further investigation, such investigations are outside the scope of the present study. The present investigation also focuses on exposed base plate connections with thick plates, such that the failure is controlled by the anchor rod. The parametric analysis is carried out using a finite

a) Deformed shape of the base plate connection including plastic strain plot.

b) Plot of plastic strain for grout and anchor rods.

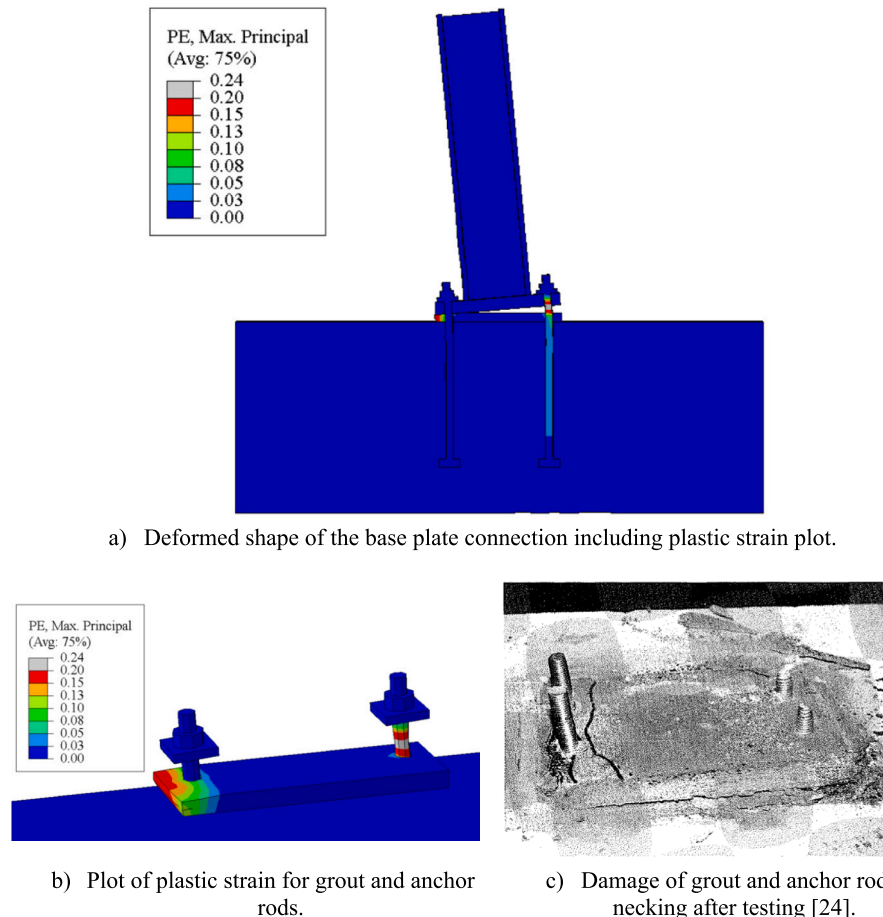c) Damage of grout and anchor rod necking after testing [24].

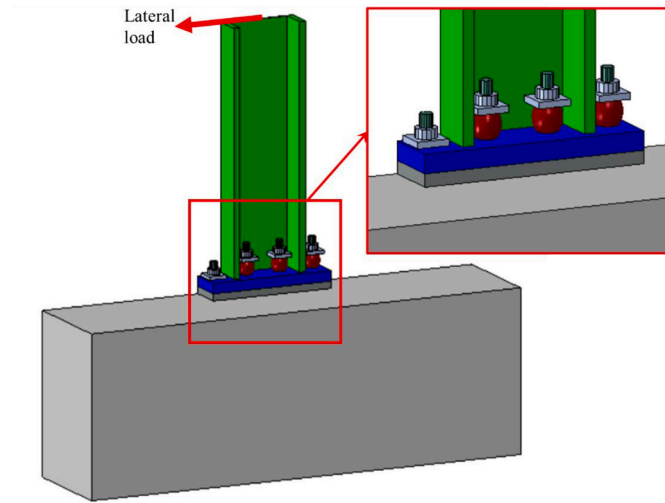**Fig. 7.** Comparison of numerical and experimental failure modes.

Fig. 8. Column base connection considered in the parametric study.

element (FE) model validated against experimental tests.

3. Development of finite element model

A 3D FE model was employed using solid elements to model the base plate connection shown in Fig. 3. The steel specimens (column and the base plate) were attached to 460 mm deep reinforced concrete pad footings with plan dimensions of 1270 mm × 610 mm. A smooth shank anchor rod with a diameter of 19 mm and an embedment length of 340 mm was used. The anchor rods were fully anchored to the foundation such that the failure mode is rod rupture rather than concrete failure. A 20 mm cement grout was used between the base plate and the concrete footing. The load was monotonically applied to the steel column by a hydraulic jack positioned at 741 mm from the top of the base plate. The tests were carried out under a force-control method [24].

The model was developed in ABAQUS/CAE [25] with an implicit solver. Due to the symmetry of the geometry and boundary conditions, only half of the specimen was modelled, with the axis of symmetry passing through the centreline of the column's web. The components of the base plate connection including base plate, anchor rods, washers, nuts, grout, footing, and column were modelled using 8-node linear

brick elements with reduced integration (C3D8R). A refined mesh was employed at locations where stress concentrations were anticipated. Several approaches have been adopted in the existing literature to model the anchor rod geometry including a uniform thread throughout the length, explicit modelling of the thread and non-thread region, and spring elements [26–30]. In the present study, the anchor rod was modelled with its full diameter throughout its length to simplify the mesh. Both geometric and material nonlinearities were introduced during the analysis.

3.1. Materials

A trilinear constitutive law was used to model the anchor bolt material. The yield stress f_y = 308 MPa and ultimate stress f_u = 500 MPa were defined based on the tensile tests carried out on coupon specimens presented in [24]. With the absence of the complete stress-strain curve of the anchor bolt, several trials with various ultimate strains (corresponding to the ultimate stress) were considered until desired connection behaviour was observed. The stress-strain response of the anchor rod material is shown in Fig. 4. As previously mentioned, the present study focusses mainly on column bases with thick end plates in which the capacity is mainly controlled by the anchor rod rupture. Thus, an elastic-perfectly-plastic constitutive model was used for the base plate and column with a yield stress of 250 and 300 MPa, respectively. However, the plastic strain of the assembly was monitored during the analysis to ensure that this assumption is not violated. The concrete grout and foundation pad were modelled using an elastic-perfectly-
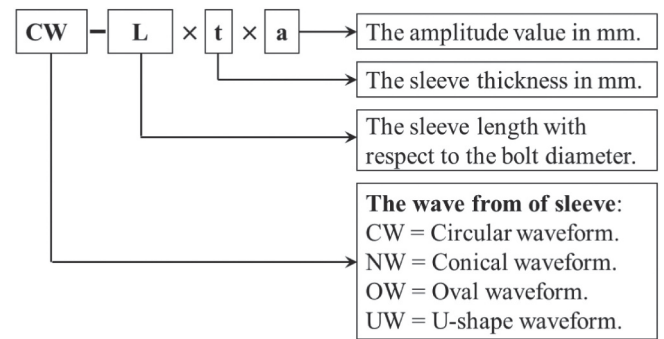

Fig. 9. Specimen identifier.

Table 1
Sleeve configurations considered in the present study and the associated geometric parameters.

	Circular waveform	Conical waveform	Oval waveform	U-shaped waveform
Geometric parameters				
3D view				
Cross-sectional view				

Table 2
Comparison between rotational and moment capacity of the standard column base connection with that of the sleeved connection.

Model	R^1 (rad)	M^2 (kN.m)	K^3 (kN.m/rad)	R_{sle}/R_{std}^4	M_{sle}/M_{std}^5	K_{sle}/K_{std}^6
Standard connection	0.167	180.19	10340	-	-	-
CW-1d×5.5×3	0.195	191.31	10216	1.17	1.06	0.99
CW-1d×5.5×6	0.193	191.39	10330	1.15	1.06	1.00
CW-1d×5.5×8	0.182	191.50	10323	1.09	1.06	1.00
CW-1.5d×5.5×3	0.195	191.31	10216	1.17	1.06	0.99
CW-1.5d×5.5×7	0.195	191.83	10158	1.17	1.06	0.98
CW-1.5d×5.5×8	0.235	195.09	9998	1.41	1.08	0.97
CW-1.5d×5.5×9	0.250	191.26	10103	1.50	1.06	0.98
CW-2d×5.5×3	0.188	191.45	10087	1.12	1.06	0.98
CW-2d×5.5×8	0.207	191.94	10009	1.24	1.07	0.97
CW-2d×5.5×9	0.262	195.51	9968	1.57	1.08	0.96
CW-2d×5.5×10	0.289	188.42	9922	1.73	1.05	0.96
NW-1.5d×5.5×3	0.194	191.33	10216	1.16	1.06	0.99
NW-1.5d×5.5×4	0.204	191.64	10194	1.22	1.06	0.99
NW-1.5d×5.5×5	0.241	197.00	10169	1.44	1.09	0.98
NW-1.5d×5.5×6	0.248	197.14	10131	1.49	1.09	0.98
OW-1.5d×5×20	0.256	189.70	8027	1.53	1.05	<mark>0.78</mark>
OW-1.5d×6×19	0.240	190.61	8714	1.44	1.06	0.84
OW-1.5d×7×18	0.224	191.94	9136	1.34	1.07	0.88
OW-2d×6×19	0.309	185.97	7870	1.85	1.03	<mark>0.76</mark>
OW-2d×7×18	0.289	193.18	8405	1.73	1.07	0.81
OW-2d×8×17	0.212	190.87	8840	1.27	1.06	0.85
OW-2d×9×16	0.194	191.08	9259	1.16	1.06	0.90
UW-1.5d×6×14.5	0.267	189.84	6944	1.60	1.05	<mark>0.67</mark>
UW-1.5d×8×12.5	0.230	189.63	8638	1.38	1.05	0.84
UW-1.5d×10×10.5	0.196	191.35	9709	1.17	1.06	0.94
UW-2d×8×17.5	0.289	189.63	7190	1.73	1.05	<mark>0.70</mark>
UW-2d×10×15.5	0.258	190.70	8745	1.54	1.06	0.85
UW-2d×12×13.5	0.205	191.64	9420	1.23	1.06	0.91

[1]R is the ultimate rotation at the strength of the connection when degraded by 20% from its capacity.
[2]M is the bending moment capacity of the connection.
[3]K is the initial stiffness of the connection.
[4]R_{sle} and R_{std} are the ultimate rotation of the sleeved and standard connection, respectively.
[5]M_{sle} and M_{std} are the ultimate bending moment of the sleeved and standard connection, respectively.
[6]K_{sle} and K_{std} are the initial stiffness of the sleeved and standard connection, respectively.
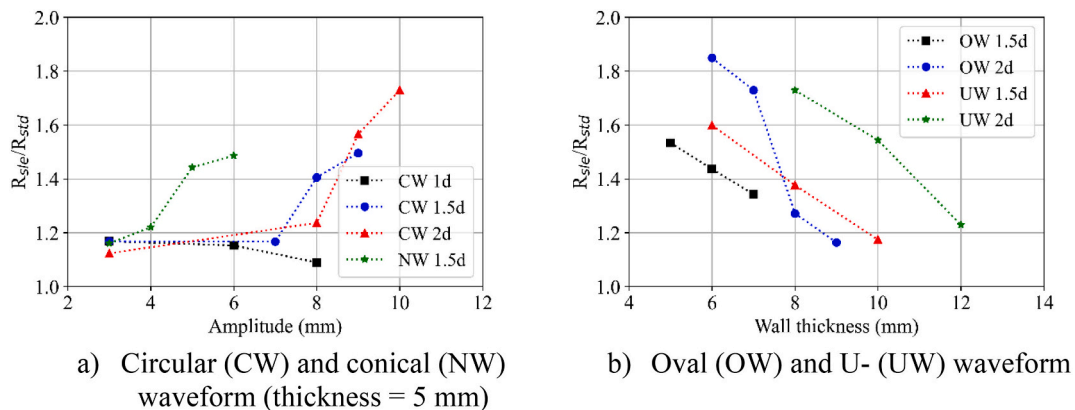

a) Circular (CW) and conical (NW) waveform (thickness = 5 mm)

b) Oval (OW) and U- (UW) waveform

Fig. 10. Comparison between rotational stiffness for the sleeved and the standard connection.

a) Moment-rotation response

b) CW-1dx5.5x3

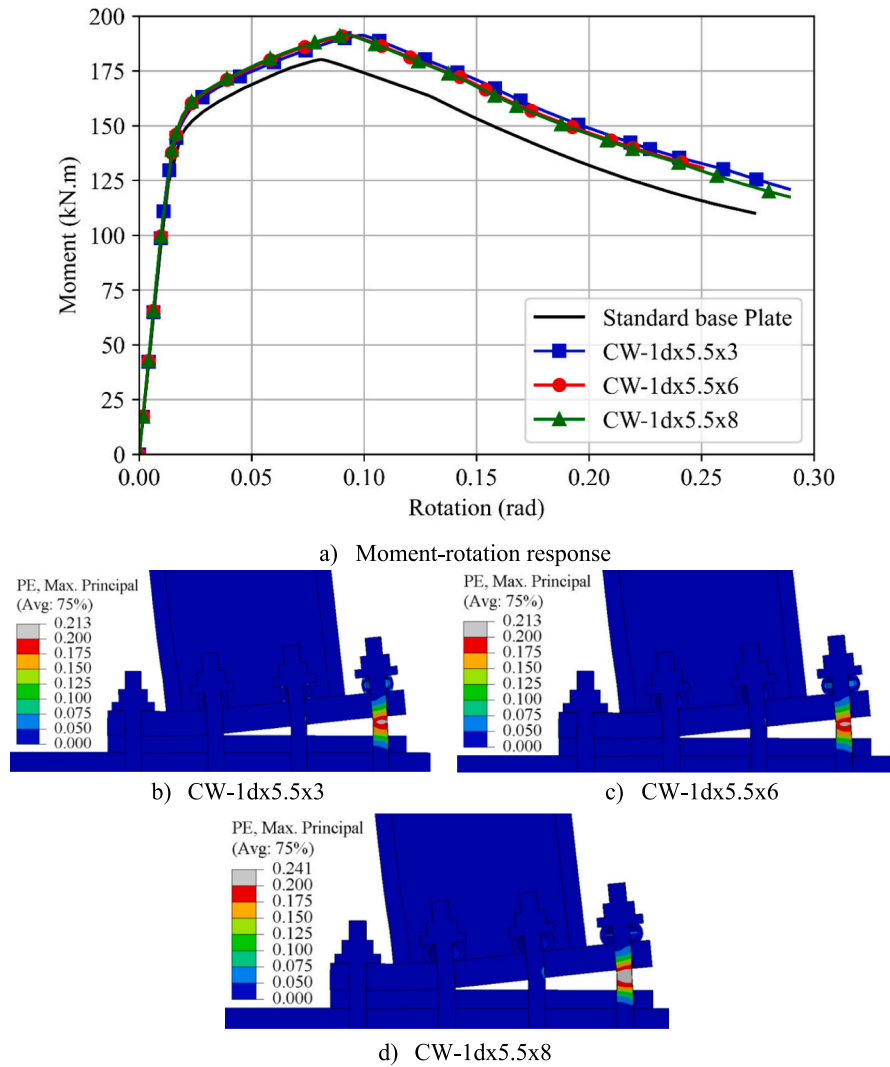c) CW-1dx5.5x6

d) CW-1dx5.5x8

Fig. 11. Behaviour of the base plate with circular waveform sleeves of length **1d** and various amplitudes.

plastic constitutive model with a compressive strength of 25 MPa [31]. It should be noted that no damage or cracking was observed in the concrete footing during the tests [24]. Thus, it was considered that the elastic-perfectly-plastic constitutive model can capture the behaviour of the foundation pad while the damage in the grout could be evaluated through the plastic deformations, as discussed later in Section 4.2. The true stress σ_T and true strain ε_T were obtained based on the well-known relations $\sigma_T = \sigma_E (1 + \varepsilon_E)$ and $\varepsilon_T = \ln (1 + \varepsilon_E)$ where σ_E is the engineering stress and ε_E is the engineering strain.

3.2. Interaction

Previous experimental tests on base plate connections concluded that the bond between the anchor rod and the concrete fails at an early stage of the load application [7,32]. Therefore, it was assumed that the tensile force resisted by the anchor plate from the onset of loading neglected the bond strength. Surface-to-surface interactions with a 0.2 friction coefficient were assigned between the anchor rod and the concrete, the anchor rod and the base plate, the bottom surface of the base plate and the top surface of the concrete grout, the anchor plate and the concrete footing and finally the washer and the base plate. A sensitivity study with friction coefficients ranging from 0.2 to 0.6 was carried out and it was found that the effect of the friction coefficient on the connection behaviour was negligible.

Previous investigations on exposed column bases concluded that the surface between the parts where no gaps or sliding is expected can be modelled monolithically [10]. Thus, surfaces between the grout and the concrete footing, the anchor rod and the nut, the nut and the washer and the anchor rod and the anchor plate were simulated as monolithic (i.e., separation is not allowed during the analysis). Further, the surface between the column and the base plate was considered as monolithic since the welds did not experience any cracking during the tests [24].

3.3. Boundary conditions and loading protocol

For the experimental tests described in the beginning of Section 3, a force control method was used, this resulted in terminating the test at the peak capacity of the connection, thus the descending post-peak curve was not recorded. However, a displacement control method was employed in the numerical analysis because of the high convergence rate and the ability to record the post-peak response. No axial load was considered during the experimental test and accordingly in the FE analysis. The movement of the bottom surface of the foundation was prevented in all three directions to simulate the experimental test. Symmetrical boundary conditions were assigned at the centre of the model to simulate the behaviour of the full model.
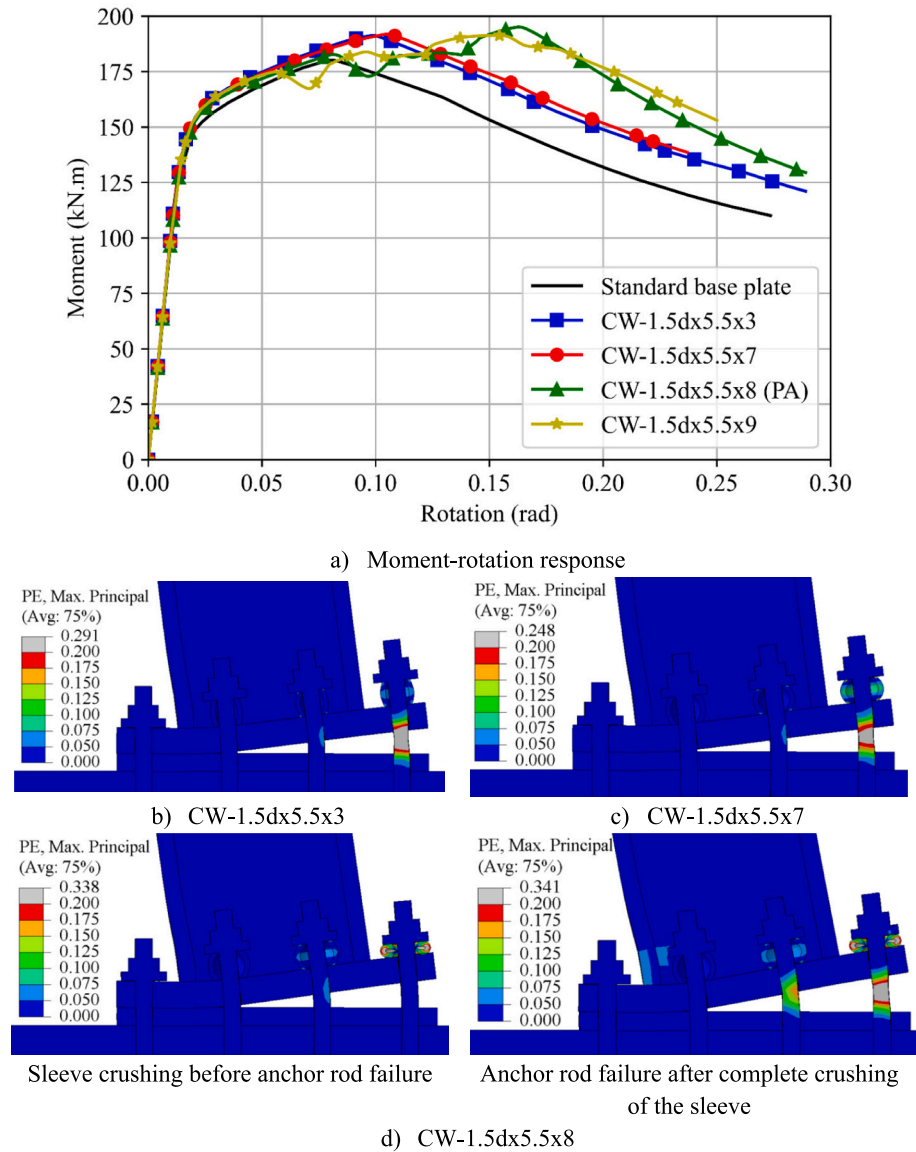
a) Moment-rotation response

b) CW-1.5dx5.5x3

c) CW-1.5dx5.5x7

Sleeve crushing before anchor rod failure

Anchor rod failure after complete crushing of the sleeve

d) CW-1.5dx5.5x8

Fig. 12. Behaviour of the base plate with circular waveform sleeves of length **1.5d** and various amplitudes.

4. Validation of FE models

4.1. Single sleeve model

Due to the expected importance of the sleeve in controlling the rotational capacity of the base plate, a single sleeve was fabricated and tested under compression to complete crushing. The sleeve's axial displacement (contraction) and the applied compression force is shown in Fig. 5 The sleeve length was 40 mm with a wall thickness of 4.7 mm as illustrated in Fig. 5. An Instron machine with a capacity of 600 kN was used for the test. The compression load was applied by the loading bar while the sleeve specimen was held on a fixed base. The load was applied monotonically under displacement control with a rate of 2.0 mm/min throughout the test duration. Fig. 5(c) shows the load-displacement behaviour of the test results compared with the FE model. The recorded sleeve capacity was 226 kN at a contraction of 7.5 mm followed by gradual decrease in the load to a contraction of 27 mm at which point the sleeve completely crushed between the loading bar and the fixed base of the testing machine. After the complete crushing of the sleeve, the load was rapidly increased, due to the increase in stiffness, up to 300 kN at which point the test was terminated. A trilinear stress-strain

constitutive model was used for the sleeve with the Eurocode 3 [33] nominal material properties of $f_y = 355$ MPa and ultimate stress $f_u = 510$ MPa. It is clear that the FE model can capture the sleeve behaviour during the elastic, plastic and crushing phases with a reasonable level of accuracy.

4.2. Base plate connection model

A comparison between the moment-rotation behaviour of the tested connection and the FE results is shown in Fig. 6, the dimensions of the tested specimen are illustrated in Fig. 3. The post-peak response of the tested connection is missing as a load control method was used during the experimental test; thus, the FE curve was compared with the test data up to the capacity of the connection, in addition to the failure mode. It should be noted that both Test 8F and Test 9F, noted in the legend of Fig. 6, have the same geometry as the test parameters. The FE model captures the elastic and plastic behaviour of the tested connection with acceptable accuracy. The capacity of the tested connection is 61.4 kN.m compared to 61 kN.m for the FE model.

Furthermore, the local behaviour of the assemblages was compared to the experimental test in order to verify the actual response of the
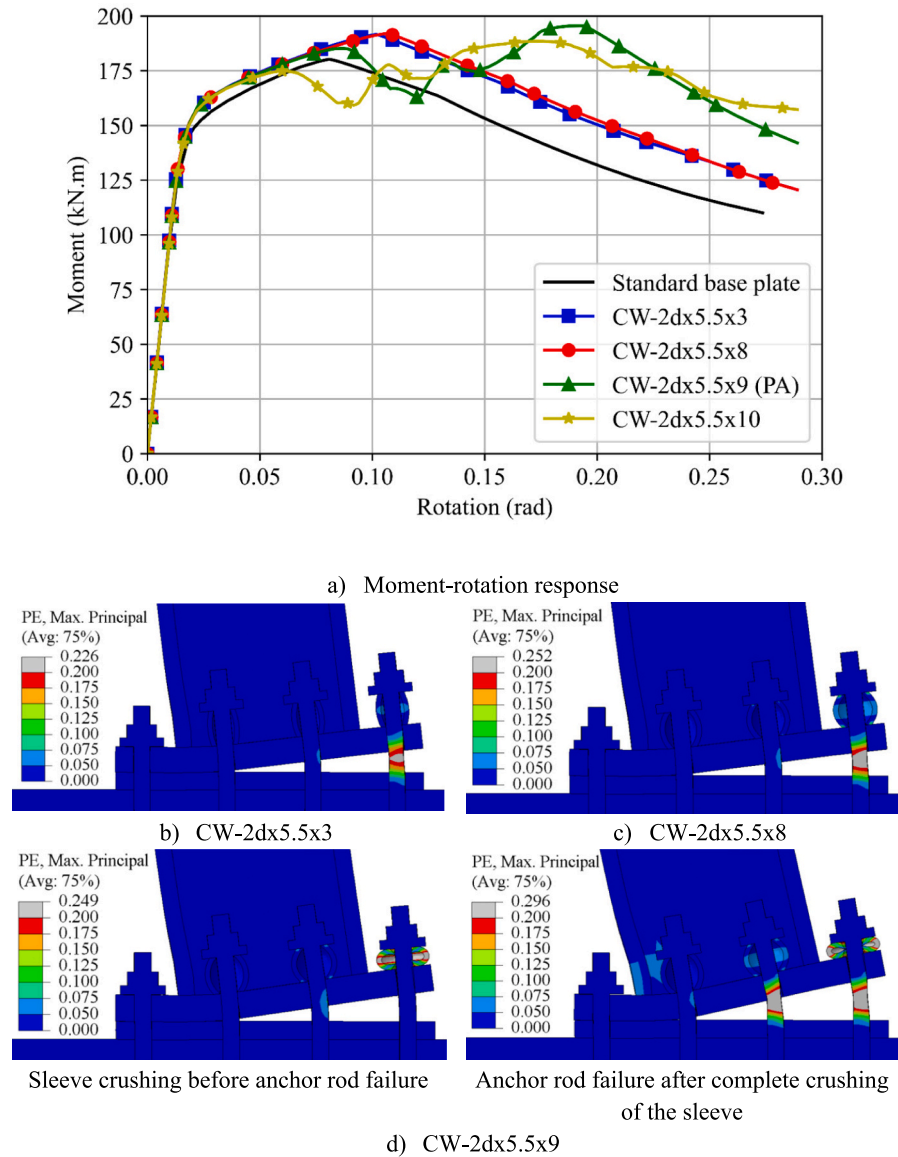
a) Moment-rotation response

b) CW-2dx5.5x3

c) CW-2dx5.5x8

Sleeve crushing before anchor rod failure

Anchor rod failure after complete crushing of the sleeve

d) CW-2dx5.5x9

Fig. 13. Behaviour of the base plate with circular waveform sleeves of length **2d** and various amplitudes.

connection. Fig. 7 depicts the deformed shape of the base plate connection as well as a comparison between the failure of the tested connection with the FE model. Grout damage was observed during the test at the extreme compression edge of the connection. The plastic strain distribution was used to compare the damage of the grout in the FE model with the experimental test. It can be observed that the damage of the grout was captured in the FE model at a similar location indicated in the test. Ultimately, the FE model failed by anchor rod necking as was observed in the test.

5. Parametric study

The number of anchor rods in the validated base plate connection model was increased to eight anchors to have a sufficient rotational capacity required for a moment resisting frame. The anchor bolt material was changed to high strength grade 8.8 to keep the study relevant to current engineering practice. The steel yield stress $f_y = 640$ MPa and ultimate stress $f_u = 800$ MPa were adopted. The column cross section was also increased to facilitate adding the sleeve without clashing with the flange. The column cross-section height was increased to 212 mm. Also, the flange thickness was increased to 18 mm to avoid local

buckling of the column cross-section. The cross section of the column was estimated based on several analysis trials with the validated model. A steel grade of S355 was considered for the sleeve material. In practice, the sleeve should be inserted between the base plate and the washer for every anchor rod in the connection. However, due to the nature of the applied load considered in this analysis, the anchor rod adjacent to the compression flange is modelled without the sleeve to reduce the computational effort, as seen in Fig. 8. Three different barrel sleeve configurations are considered as summarised in Table 1 including a circular waveform (CW), a conical waveform (NW), and an oval waveform (OW) as well as an open U-shape (UW). Specimens are identified using the system in Fig. 9.

5.1. Results and discussion

For each CW and NW sleeve type, the amplitude value was increased incrementally by 0.5 mm until reaching a sleeve capacity lower than that of the anchor rod. The amplitude value at which the sleeve capacity is less than the anchor rod capacity resulting in crushing of the sleeve between the washer and the base plate, is referred to as the plastic amplitude (PA) hereafter. Further, a sleeve with 1.0 mm amplitude
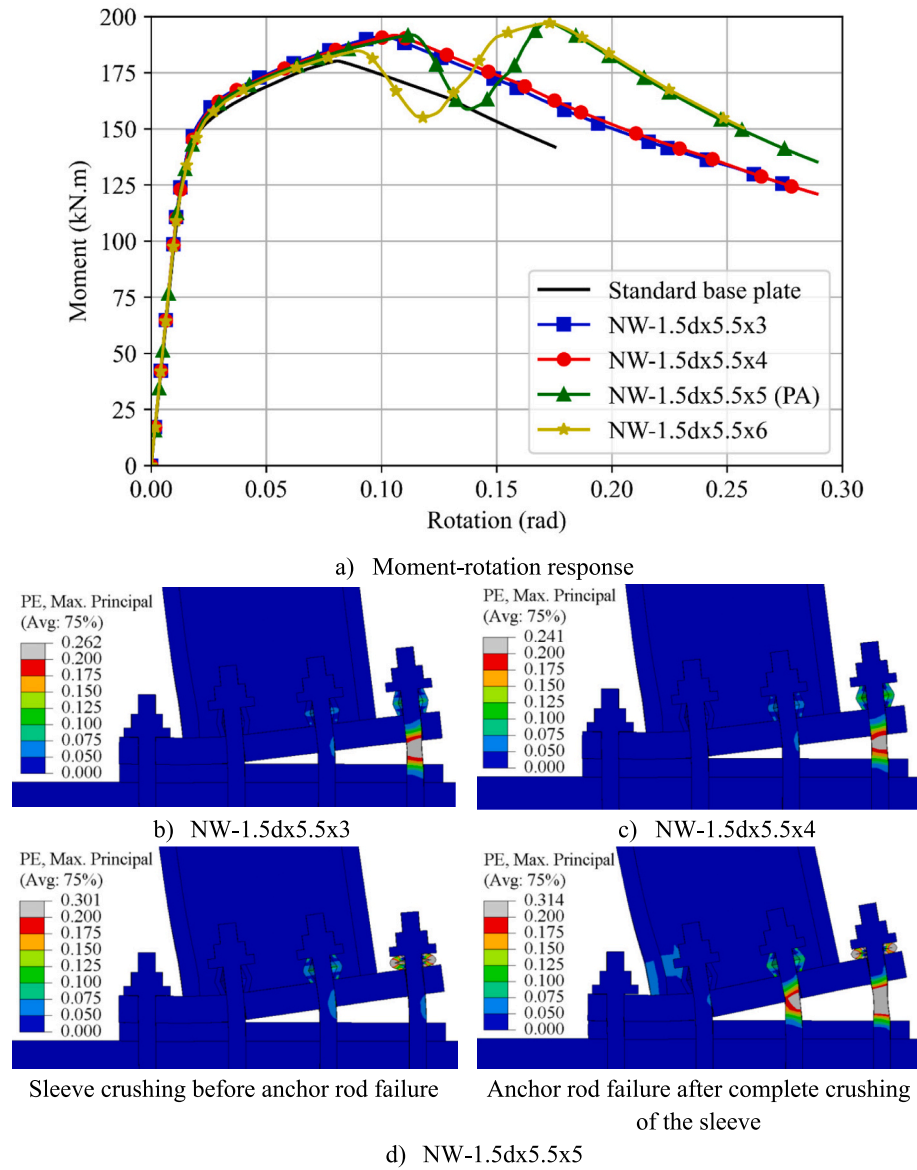
a) Moment-rotation response

b) NW-1.5dx5.5x3

c) NW-1.5dx5.5x4

Sleeve crushing before anchor rod failure

Anchor rod failure after complete crushing of the sleeve

d) NW-1.5dx5.5x5

Fig. 14. Behaviour of the base plate with conical waveform sleeves of length **1.5d** and various amplitudes.

higher than the plastic amplitude was also analysed to investigate the high amplitude effect on the behaviour of the base plate connection. Sleeve types OW and UW were also investigated with different geometric parameters. It was found that the OW and UW forms may require large plastic amplitudes resulting in spatial clashes between the sleeve and the column. Thus, it was decided to keep the outer dimensions of the sleeves constant while changing the wall thickness. Next, the results are discussed as a function of the geometry of each sleeve considering the rotational capacity, as well as the responses obtained as a function of variations in amplitude (a) and thickness (t), while comparing with the standard connection without sleeves.

Table 2 summarises the load-bearing and rotational capacity of the sleeved connection compared to the standard configuration. The moment was calculated as the lateral force multiplied by the length of the column above the surface of the base plate. The rotation was calculated as the lateral displacement divided by the column length. The rotational capacity of the connection was recorded when the load degraded by 20% from the load-bearing capacity [34]. As shown in Table 2, the sleeve device results in a slightly higher load-bearing capacity (approximately 6%) compared with the standard configuration

without sleeves; the minimum and maximum values were 185.97 kN.m and 197.14 kN.m, respectively. This increase in the load-bearing capacity was attributed to the higher ductility which improves the contribution of the inner anchor rods resisting the applied load. On the other hand, significant differences were observed in relation to the rotational capacities due to the variation of the sleeve geometry, as well as the thickness and amplitude. Fig. 10 depicts the effect of the sleeve amplitude and thickness on the rotational capacity. It is clear that the rotational capacity of the sleeved connections is higher than that of the standard configuration for all sleeves used. For CW and NW sleeves, the rotational capacity is proportional with the amplitude value (except CW 1d). In case of OW and UW sleeves, the rotational capacity is inversely proportional with the sleeve wall thickness. The initial stiffness of the sleeved and standard connections is also summarised in Table 2. The sleeved connections have comparable initial stiffnesses to that of the standard connection, the ratio of the initial stiffness ranges between 0.8 and 1.0 except for OW and UW sleeves with small wall thickness (highlighted in the table).
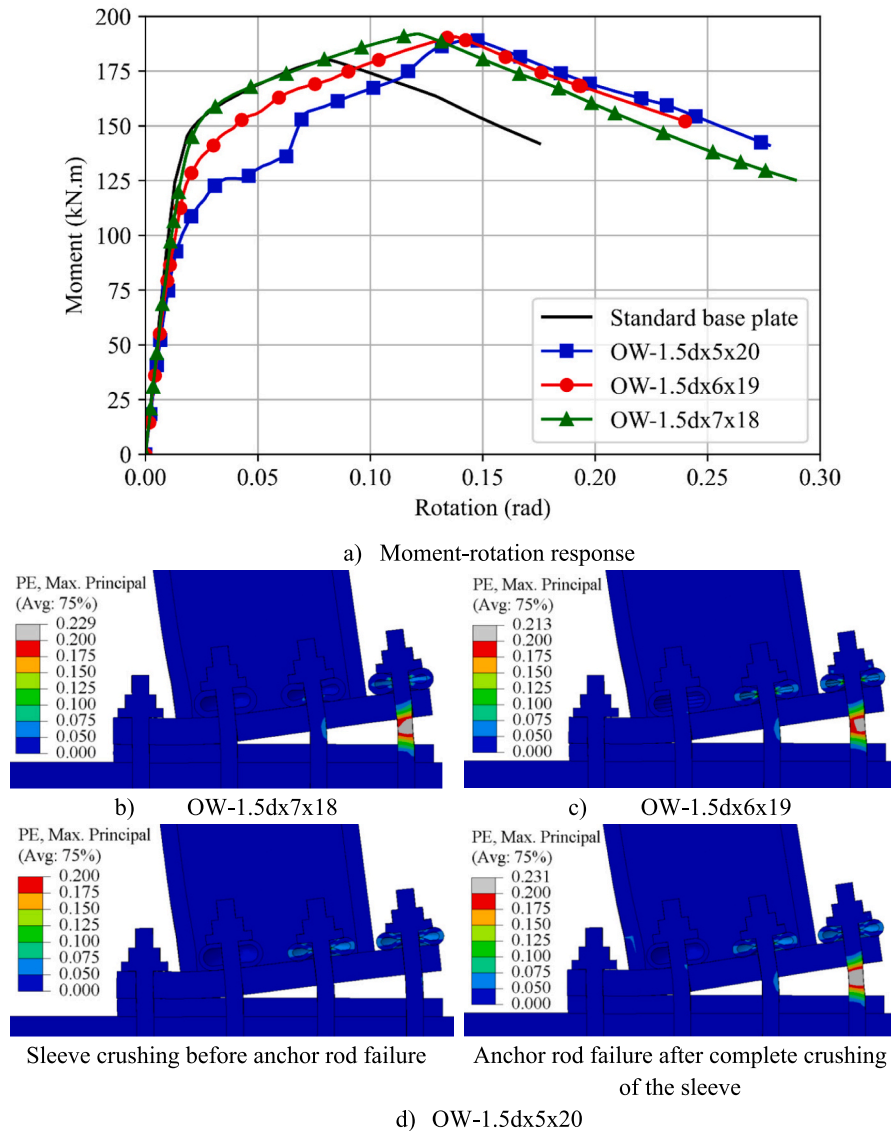
a) Moment-rotation response

b) OW-1.5dx7x18

c) OW-1.5dx6x19

Sleeve crushing before anchor rod failure

Anchor rod failure after complete crushing of the sleeve

d) OW-1.5dx5x20

Fig. 15. Behaviour of the base plate with oval waveform sleeves of length **1.5d** and various amplitudes.

5.2. Behaviour of base plate connection with circular waveform (CW) sleeves

Fig. 11 to Fig. 13 show the load-rotation relationship and plastic strain distribution for models with a length of 1.0d to 2.0d and several amplitude values, the thickness of all the sleeve was kept constant at 5.5 mm. The amplitude of each sleeve was incrementally increased by 0.5 mm until the sleeve capacity was lower than the bolt capacity and the sleeve completely crushed between the washer and the base plate. PA in the legend refers to the connection with the plastic amplitude value as noted. It is clear that the sleeves with CW depict an elastic behaviour similar to the standard base plate connection as well as slightly higher load-bearing capacity, indicating that the proposed system is compatible with existing codified elastic design approaches without modification. Referring to Table 2, for a specific sleeve length higher than 1.0d and the same thickness, the rotational capacity can be increased with a higher amplitude. Increasing the amplitude value of the sleeve results in reducing the sleeve bending capacity allowing the sleeve to experience severe plastic deformation before anchor rod failure. Fig. 12 and Fig. 13 show that the PA increases with the sleeve length, i.e., the PA for the sleeve with length 1.5d and 2.0d are 8.0 mm and 9.0 mm, respectively. A short sleeve length equal to or less than 1.0d results in a compact sleeve

that requires large PA values [21]. The short sleeve capacity was higher than that of the anchor rod, even with a large amplitude value of 8.0 mm, resulting in failure of the anchor rod without experiencing plastic deformation in the sleeve as shown in Fig. 11(b-d).

Fig. 12 shows the moment-rotation response of a sleeve with a length of 1.5d as well as the deformed shape and plastic strain distribution at failure. Referring to Fig. 12(a), the sleeve with various amplitude values depicts similar moment-rotation response within the elastic range and up to 0.06 rad. A drop in the bending moment was observed at about 0.08 rad and 0.06 rad for the sleeve with amplitude of 8.0 mm and 9.0 mm respectively, due to the initiation of sleeve crushing, which then ultimately jammed between the base plate and the washer as shown in Fig. 12(d). However, increasing the amplitude value of the sleeve beyond the PA slightly reduces the load-bearing capacity of the connection and the sleeve crushes at a lower rotation value. In comparison with the standard base plate connection, there was a minimum gain in the rotational capacity of 17% and 50%, considering the models with amplitude equal to 3 mm and 9 mm, respectively. It was observed that in the models with 3 to 7 mm amplitudes (Fig. 12(b and c)), anchor rod failure occurred before sleeve crushing resulting in a limited increase in the rotational capacity. For the models with 8 mm (Fig. 12(d)) and 9 mm amplitude, the sleeve mated with the furthest bolt from the
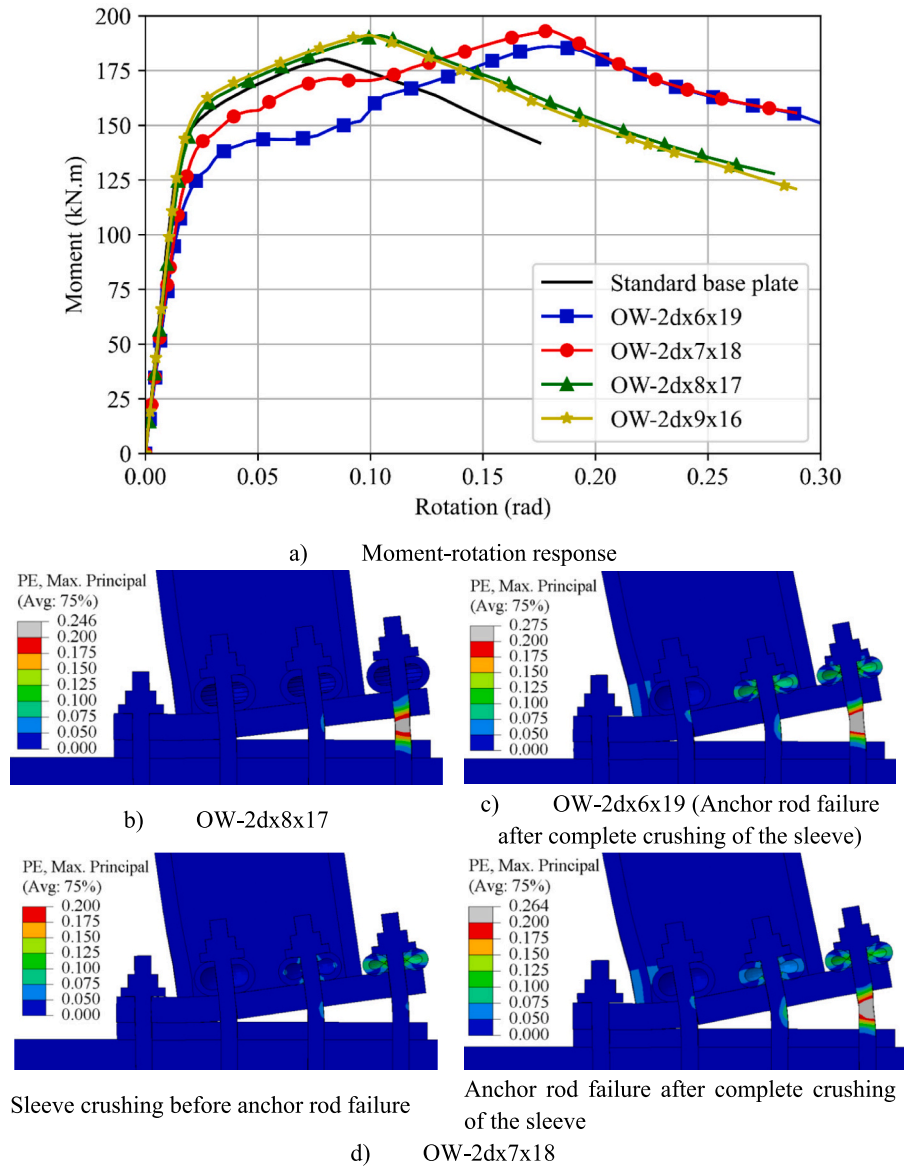
a) Moment-rotation response

b) OW-2dx8x17

c) OW-2dx6x19 (Anchor rod failure after complete crushing of the sleeve)

Sleeve crushing before anchor rod failure

Anchor rod failure after complete crushing of the sleeve

d) OW-2dx7x18

Fig. 16. Behaviour of the base plate with oval waveform sleeves of length **2d** and various amplitudes.

compression flange crushed before anchor rod failure resulting in a significant improvement in the rotational capacity.

For models with 2.0d (Fig. 13), the load-rotation relationship behaviour was similar to the 1.5d models, i.e., the greater the amplitude, the greater the rotational capacity. The PA of the 2.0d length sleeve was observed at 9.0 mm compared with 8.0 mm for the 1.5d sleeve, implying that the PA of the sleeve increases with the sleeve length. For circular sleeves with the same geometrical parameters, increasing the sleeve length results in a higher radius of curvature; this shifts the force transfer mechanism of the sleeve from combined bending and membrane action to membrane action alone and may result in higher sleeve capacity, which requires higher PA value. The maximum values of the rotational capacity were 0.188 rad and 0.289 rad, for the 3 mm and 10 mm amplitude models, respectively. This means that there has been an increase in the rotational capacity of a minimum of 12% and a maximum of 73% compared to the standard connection. Fig. 13(c) shows the complete crushing of the sleeve did not occur for the sleeve with 8.0 mm amplitude resulting in failure of the anchor rod before the sleeve and in limited rotation capacity. For the sleeve with an amplitude of 9 mm (Fig. 13(d)), sleeve crushing was observed before the anchor rod failure,

which significantly enhanced the rotational capacity of the connection as shown in Fig. 13(a).

5.3. Behaviour of base plate connection with conical waveform (NW) sleeves

Fig. 14 shows the load-rotation relationship and plastic strain distributions of the base plate connection with NW sleeves having a length of 1.5d and various amplitudes. In a comparable way to the CW sleeves, there were no differences to the standard connection in the elastic regime. All NW sleeve models had a rotational capacity higher than the standard connection. For the 3 mm amplitude model, the rotational capacity was 0.194 rad. On the other hand, the model with amplitude equal to 6 mm presented a rotational capacity equal 0.248 rad. In comparison with the standard connection, there was a minimum and maximum increase of 16% and 49%, respectively, in rotational capacity. However, NW sleeves exhibit a sudden drop in the moment at about 0.12 rad and 0.09 rad for amplitudes of 5.0 mm and 6.0 mm, respectively, due to the early sleeve crushing, as shown in Fig. 14(d). This sudden drop in the capacity is not preferred in engineering practice as it
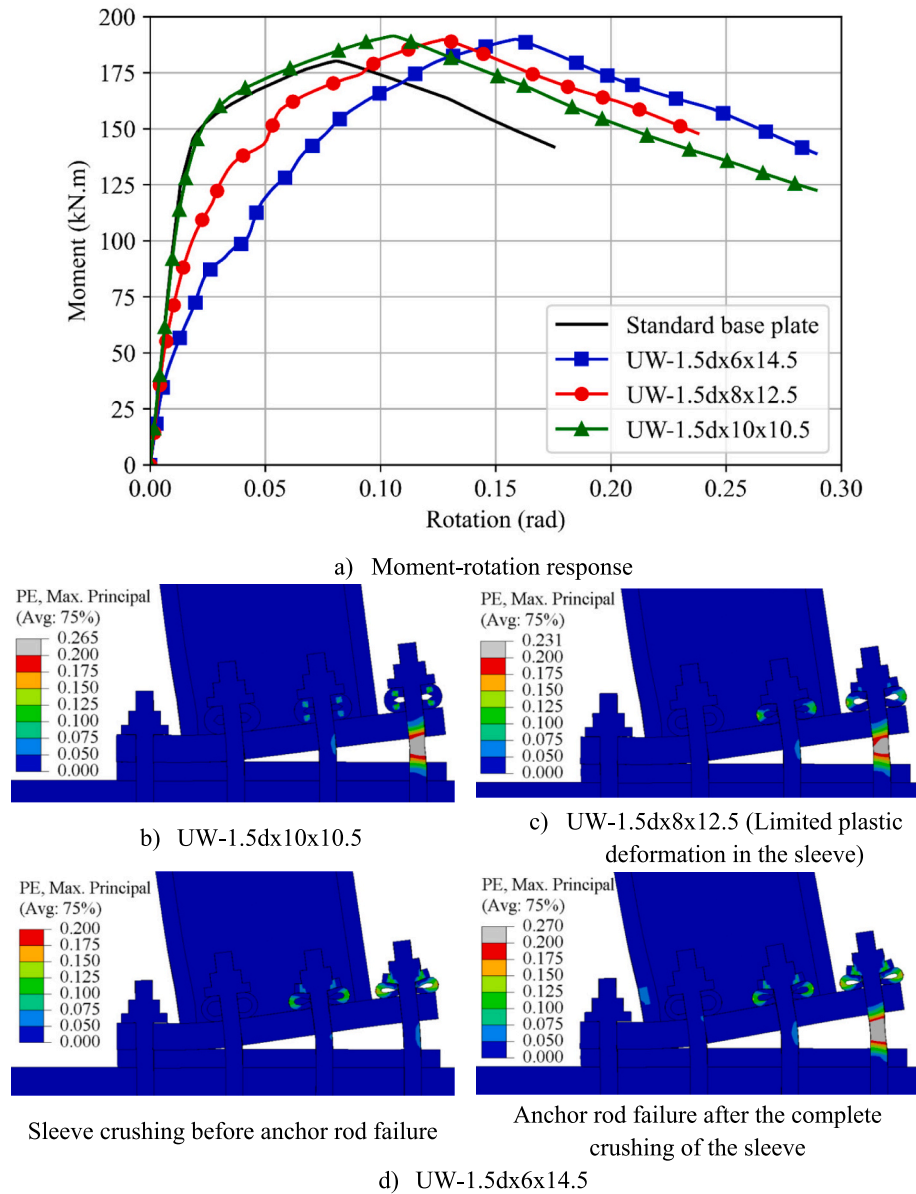
a) Moment-rotation response

b) UW-1.5dx10x10.5

c) UW-1.5dx8x12.5 (Limited plastic deformation in the sleeve)

Sleeve crushing before anchor rod failure

Anchor rod failure after the complete crushing of the sleeve

d) UW-1.5dx6x14.5

Fig. 17. Behaviour of the base plate with U-shaped sleeves of length **1.5d** and various amplitudes.
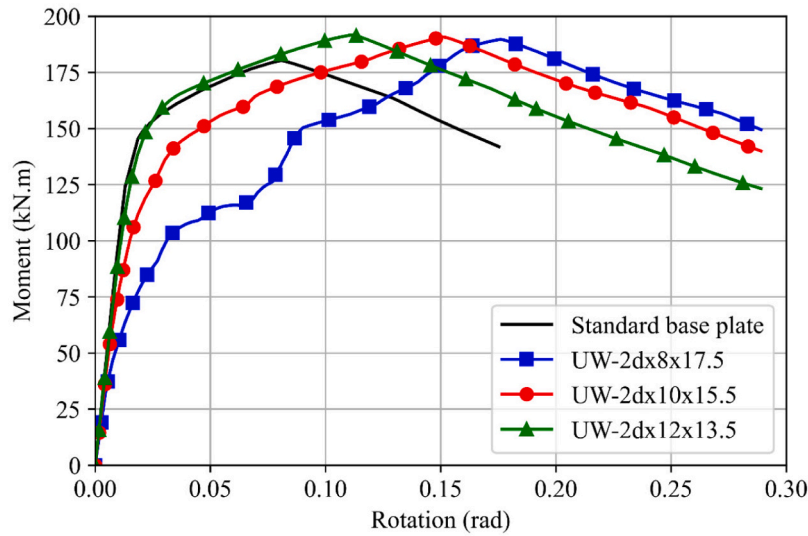
may degrade the load redistribution capabilities, thus it was decided to exclude NW sleeves from further investigations.

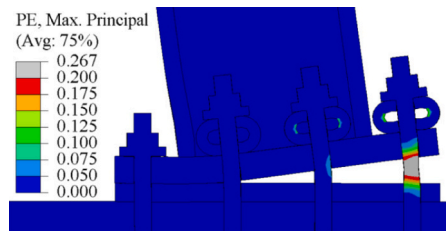### 5.4. Behaviour of base plate connection with oval waveform (OW) sleeves

The results of base plate connections with OW sleeves are shown in Fig. 15 and Fig. 17 for sleeves with a length of 1.5d and 2.0d, respectively. It is clear that differences in the elastic behaviour were observed when compared to the standard connection (Fig. 15(a) and Fig. 17(a)) depending on the geometrical parameters of the sleeve. In this sleeve type, the outer middle diameter was kept constant for all sleeves while the thickness was varied. For example, the sum of the sleeve amplitude and the thickness in the legend of Fig. 15(a) and Fig. 17(a) is constant (= 25 mm). It was noted that the lower the thickness, the higher the stress levels in the sleeves, causing the nonlinear regime to occur at lower values of rotation compared with the CW sleeve. Although the nonlinear regime may occur prematurely, the rotational capacity and strength remained higher than that of the standard connection. Fig. 15(b-d) and Fig. 17(b-d) depict the plastic strain distribution on the deformed shape

of the base plate connection with 1.5d and 2.0d, respectively. It was noted that the sleeve with a length of 1.5d completely crushed at a thickness of 5 mm while 2.0d crushed at a thickness of 6 mm.
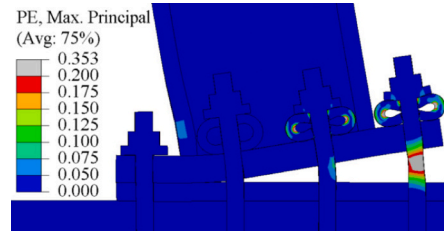
Comparing moment-rotation behaviour of OW sleeves with both CW and NW sleeves shows that OW sleeves result in a more stable response under the applied load. CW and NW sleeves experience several drops in bending moment within the plastic region of the moment-rotation response while the bending moment of connections with OW sleeves increase steadily with the rotation within the plastic region. A sudden increase in the moment was experienced at about 0.06 rad 0.09 rad for OW-1.5dx5x20 and OW-2dx6x19 respectively, due to the complete crushing of the sleeves on the tension side. It should be pointed out that two sleeves were completely crushed and jammed between the washer and the base plate for the connection with OW sleeves (see Fig. 15(d) and Fig. 17(d)) as opposed to one sleeve for connections with CW sleeves (Fig. 12(d) and Fig. 13(d)).
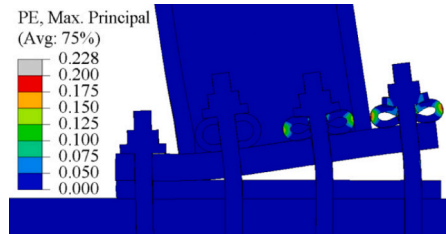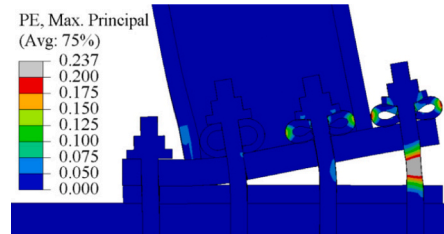
a) Moment-rotation response

b) UW-2dx12x13.5

c) UW-2dx10x15.5 (Limited plastic

deformation in the sleeve)

Two sleeves crushing before anchor rod

failure

Anchor rod failure after complete crushing

of the sleeve

d) UW-2dx8x17.5

Fig. 18. Behaviour of the base plate with U-shaped sleeves of length **2d** and various amplitudes.

5.5. Behaviour of base plate connection with U-shape waveform (UW) sleeves

The moment-rotation response and plastic strains for models with length of 1.5d and 2.0d, are shown in Fig. 17 and Fig. 18, respectively. Connection models UW-1.5dx10x10.5 and UW-2dx12x13.5 revealed an elastic response similar to that of the standard connection. However, the elastic behaviour started prematurely with reducing the sleeve thickness. This phenomenon can be determined as a function of the amplitude and thickness, that is, with decreasing thickness and increasing amplitude, the stress and strain levels increased considerably. However, this behaviour did not change the increase in the rotational capacity of models with sleeves. In this context, there was a minimum and maximum increase of 17% and 73% in the rotational capacity for the connection with U-shaped sleeves (see table Table 2) in comparison with the standard connection model. Regarding the plastic strains, as shown

in Fig. 17(b-d) and Fig. 18(b-d), it was observed that the smaller the thickness and the greater the amplitude of the sleeves, the greater the levels of plastic deformation, which causes sleeve crushing before anchor rod rupture resulting in higher rotational capacity.

Connections with U-shaped sleeves produce a similar response to that with OW sleeves in which the two sleeves on the tension side are completely crushed and jammed between the washer and the end plate before the anchor rod ruptures. Furthermore, the connections with the U-shaped sleeves show stable moment-rotation response as the sudden drop in bending moment was absent within the plastic region of moment-rotation curve. However, the connection with the U-shaped sleeves depicts higher flexible response compared with the OW sleeves. Comparison of Fig. 16(a) and Fig. 18(a) for OW and U-shaped sleeves respectively shows that for sleeves with the same length, the latter sleeve type presents lower stiffness and earlier plastic response when the sleeve capacity is lower than the bolt capacity.
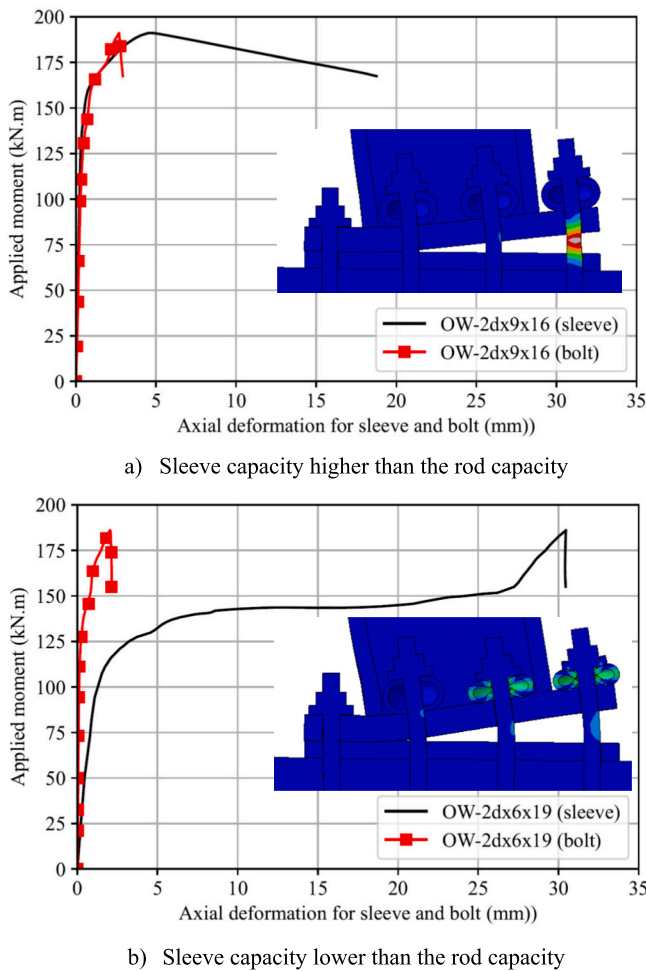
a) Sleeve capacity higher than the rod capacity

b) Sleeve capacity lower than the rod capacity

Fig. 19. Axial deformation and plastic strain plot of the bolt and sleeve under the applied moment.

6. Discussion

Fig. 19 compares the axial deformation in the bolt and the sleeve when various OW sleeve capacities were used; a sleeve capacity higher than that the anchor rod was adopted in Fig. 19(a) (referred to as a strong sleeve) while a sleeve capacity lower than that the anchor rod was adopted in Fig. 19(b) (referred to as a weak sleeve). It should be noted that the vertical axis in Fig. 19 represents the applied moment on the connection. When a strong sleeve is used, the sleeve undergoes limited deformation before the anchor rod ruptures resulting in a marginal improvement in rotational capacity (16% greater than the standard configuration as shown in Table 2). The anchor rod failed at about 2.5 mm axial deformation causing the connection to achieve its load-bearing capacity at limited sleeve axial deformation at about 5.0 mm (see Fig. 19(a)). Reducing the sleeve capacity such that the sleeve fails before the anchor rod results in significant plastic deformation before the anchor rod ruptures (see Fig. 19(b)) and hence higher rotational capacity (85% greater than the standard configuration as shown in Table 2). Fig. 19(b) shows axial deformation of a weak OW sleeve under the applied load. The sleeves exhibit significant plastic deformation at an applied load of ~140 kN.m and eventually crush between the end plate and the washer before failure of the bolt. For example, the axial deformation at 150 kN is 25 mm for the weak sleeve. The applied moment attains the peak value either when the sleeve jams between the washer and the end plate, as for the weak sleeve, or when the force in the sleeve exceeds the anchor rod capacity, providing that the sleeve capacity is higher than the bolt capacity, as for the strong sleeve. The

Table 3
Performance ratios of the sleeved connection normalised by that of the standard connection.

Model	$M_{y,sle}/M_{y,std}$	$\theta_{y,sle}/\theta_{y,std}$	$M_{u,sle}/M_{u,std}$	R_{sle}/R_{std}
CW-1d × 5.5 × 3	1.06	1.03	1.06	1.17
CW-1d × 5.5 × 6	1.06	1.03	1.06	1.15
CW-1d × 5.5 × 8	1.06	1.03	1.06	1.09
CW-1.5d × 5.5 × 3	1.04	1.03	1.06	1.17
CW-1.5d × 5.5 × 7	1.04	1.03	1.06	1.17
CW-1.5d × 5.5 × 8	1.04	1.03	1.08	1.41
CW-1.5d × 5.5 × 9	1.04	1.03	1.06	1.50
CW-2d × 5.5 × 3	1.03	0.99	1.06	1.12
CW-2d × 5.5 × 8	1.03	0.99	1.07	1.24
CW-2d × 5.5 × 9	1.03	0.99	1.08	1.57
CW-2d × 5.5 × 10	1.03	0.99	1.05	1.73
NW-1.5d × 5.5 × 3	1.00	1.06	1.06	1.16
NW-1.5d × 5.5 × 4	1.00	1.06	1.06	1.22
NW-1.5d × 5.5 × 5	1.00	1.06	1.09	1.44
NW-1.5d × 5.5 × 6	1.00	1.06	1.09	1.49
OW-1.5d × 5 × 20	**0.73**	**0.68**	1.05	1.53
OW-1.5d × 6 × 19	0.93	0.96	1.06	1.44
OW-1.5d × 7 × 18	0.96	1.02	1.07	1.34
OW-2d × 6 × 19	**0.86**	**0.78**	1.03	1.85
OW-2d × 7 × 18	0.94	0.93	1.07	1.73
OW-2d × 8 × 17	1.04	1.07	1.06	1.27
OW-2d × 9 × 16	1.04	1.07	1.06	1.16
UW-1.5d × 6 × 14.5	**0.27**	**0.36**	1.05	1.60
UW-1.5d × 8 × 12.5	**0.61**	**0.77**	1.05	1.38
UW-1.5d × 10 × 10.5	0.95	0.97	1.06	1.17
UW-2d × 8 × 17.5	**0.41**	**0.03**	1.05	1.73
UW-2d × 10 × 15.5	**0.76**	**0.68**	1.06	1.54
UW-2d × 12 × 13.5	0.95	0.99	1.06	1.23

Where:
- $M_{y,sle}$ and $M_{y,std}$ are the yielding moment of the sleeved and standard connection, respectively.
- $\theta_{y,sle}$ and $\theta_{y,std}$ are the yielding rotation of the sleeved and standard connection, respectively.
- R_{sle} and R_{std} are the ultimate rotation of the sleeved and standard connection, respectively.

optimal behaviour of the base plate connection is obtained when the sleeve experiences significant plastic deformation and completely crushes between the washer and the end plate before failure of the anchor rod i.e. when the weak sleeve is adopted. The sudden drop in the load at about 30 mm (Fig. 19(b)) was due to the complete crushing of the sleeve resulting in the axial deformation of the sleeve being zero.

The performance ratios of the sleeved connection with respect to that of the standard connection are summarised in Table 3, the definition of the terms is listed at the end of the table. The yield moment and rotation are approximately defined at the point where a significant change of the initial stiffness of the hysteretic curve is observed [35,36]. The ultimate rotation is defined at the point where the strength of the connection is degraded by 20% from its capacity. Referring to the table, the sleeve device has a slight effect on the yield moment and rotation of the connection as the change in the performance ratios for the sleeved connection to that of the standard connection is less than 10%, except for OW and UW sleeves with thin walls (bolded in the table). As aforementioned, the capacity of the sleeved connection is slightly higher than the standard connection for all sleeve types.

7. Limitations

In the present study, nominal material properties for mild steel grade S355 were used for the sleeve. However, the strength of the supplied material is frequently higher than the nominal value. If the sleeve geometric parameters are defined based on the nominal value, its ultimate capacity would be higher than the anchor rod capacity leading to the anchor rod failing without developing sufficient plastic deformation in the sleeve. Previous study of the sleeve device with beam end-plate connections concluded that the higher the material strength, the lower

the rotational capacity, however the behaviour can be converged at a specific strength margin. Thus, stringent control on the sleeve material properties should be considered to limit this implication. However, further analysis is required to define the margin for the increase in the material strength and a possible factor of safety.

The primary objective of the present study is to demonstrate the concept of the proposed sleeve device with the base plate. Consequently, various parameters for future investigation remain including: i) the behaviour of the sleeved connection where additional failure modes occur such as concrete failure modes, base plate and weld cracking ii) the effect of tension force in the column on the sleeve response; iii) the effect of friction between the sleeve and the steel plates on the sleeve capacity, iv) and the effect of anchor rod pre-loading on the sleeve response. Subsequent work will include experimental investigations, so that the metallurgical failure modes that can arise from microscopic defects can be taken into account. This will inform the development of analytical models and design methodologies for practical applications. Further, it should be noted that the investigations in the present study were carried out under monotonic loading which cannot be applied directly to connections subjected to dynamic loading such as seismic actions without further studies. Existing studies on beam-column bolted connections conclude that the ductility and the energy dissipation capabilities of the connection increase for higher loading rates [37]. To the authors' knowledge, there are no similar studies in the literature that compare the behaviour of column bases under dynamic and static loading.

The geometrical parameters of the sleeve can be defined based on detailed numerical or experimental analysis. However, Shaheen et al. [21] discussed the geometrical parameters of the sleeve with circular waveform and proposed a mathematical equation to evaluate the optimum geometry such that the sleeve capacity would be less than that of the bolt. The FE models developed in the present study do not consider the possibility of failure of the washer. Failure of the washer may result in the sleeve disengaging from the washer, which may lead to the premature failure of the connection. Shaheen et al. [21] proposed an analytical equation to evaluate the washer dimensions such that the premature failure of the washer can be avoided before crushing of the sleeve. However, further investigation is required for other sleeve types and also the adoption of thick washers.

8. Concluding remarks

This paper studies a newly proposed sleeve system for steel column exposed base connections A finite element model was developed and validated against meso-scale experimental tests. A parametric study was then conducted, considering four types of sleeve geometries: circular (CW), conical (NW), oval (OW) and U-shaped (UW) waveforms. The geometric parameters of the sleeves, such as length, thickness and amplitude were varied. The results were compared with the standard connection to investigate the ductility of the proposed system. All conducted finite element models presented values of resistance, lateral displacements and rotations higher than the standard connection, demonstrating that the proposed system improved the steel column base connections. For each sleeve type and geometry examined, the following can be concluded:

- Connections with circular waveform sleeves showed similar linear elastic behaviour when compared to the standard connection. For connections with a sleeve length of 1.0d, there were insignificant differences in the load-rotation relationship with the amplitude variation. For the 1.5d and 2.0d models, the greater the amplitude, the greater the rotational capacity. Sleeve crushing can occur before anchor rod failure at a specific plastic amplitude (PA) value. The PA values were verified at 9 mm and 10 mm, for the sleeves of 1.5d and 2.0d, respectively, when the sleeve thickness is 5.5 mm. These values provided greater rotational capacity.

- For oval waveform sleeves compared to the standard connection, there were significant differences in the elastic behaviour. This was due to the variation in thickness. The lower the thickness of the sleeve wall, the lower the limit load of the elastic behaviour. With the increase in the amplitude, there was an increase in the rotations.

- U-shaped waveform sleeves showed similar elastic behaviour to sleeves with an oval waveform, that is, the lower the thickness of the 1.5d and 2.0d models, the lower the limit load of the elastic behaviour. By increasing the amplitude, rotations also increased. For thickness values less than 12 mm, crushing of the sleeve was observed before the anchor rod failure.

CRediT authorship contribution statement

Mohamed A. Shaheen: Conceptualization, Formal analysis, Writing - original draft. **Konstantinos Daniel Tsavdaridis:** Writing - review & editing. **Felipe Piana Vendramell Ferreira:** Writing - review & editing. **Lee S. Cunningham:** Writing - review & editing.

Declaration of Competing Interest

The authors declare that they have no known competing financial interests or personal relationships that could have appeared to influence the work reported in this paper.

Data availability

Data will be made available on request.

References

[1] J.M. Fisher, L.A. Kloiber, Steel Design Guide 1: Base Plate and Anchor Rod Design, AISC Steel Des Guid Ser, 2006.

[2] V. Gioncu, F. Mazzolani, Seismic Design of Steel Structures, 2013.

[3] BSI, BS EN 1998:2014 - Design of structures for earthquake resistance. BSI, London, UK, 2014, https://doi.org/10.1007/978-3-642-41714-6_51761.

[4] ANSI/AISC 341–16, Seismic Provisions for Structural Steel Buildings, 2016.

[5] S. Kishiki, X. Yang, T. Ishida, N. Tatsumi, S. Yamada, Experimental study of concrete breakout failure mechanism in an exposed column base with a foundation beam, Eng. Struct. (2021) 243, https://doi.org/10.1016/j.engstruct.2021.112661.

[6] X. Yang, S. Kishiki, Evaluation of ultimate strength of exposed column bases considering the bearing stress of foundation concrete, Eng. Struct. 268 (2022), 114712, https://doi.org/10.1016/j.engstruct.2022.114712.

[7] I. Gomez, A. Kanvinde, G.G. Deierlein, Exposed Column Base Connections Subjected to Axial Compression and Flexure, AISC Final Report Chicago, 2010.

[8] C.A. Trautner, T. Hutchinson, P.R. Grosser, J.F. Silva, Effects of detailing on the cyclic behavior of steel baseplate connections designed to promote anchor yielding, J. Struct. Eng. (2016), https://doi.org/10.1061/(asce)st.1943-541x.0001361.

[9] K.D. Tsavdaridis, M.A. Shaheen, C. Baniotopoulos, E. Salem, Analytical approach of anchor rod stiffness and steel base plate calculation under tension, Structures 5 (2016) 207–218.

[10] M.A. Shaheen, K.D. Tsavdaridis, E. Salem, Effect of grout properties on shear strength of column base connections: FEA and analytical approach, Eng. Struct. 152 (2017) 307–319.

[11] T. Falborski, P. Torres-Rodas, F. Zareian, A. Kanvinde, Effect of base-connection strength and ductility on the seismic performance of steel moment-resisting frames, J. Struct. Eng. (2020), https://doi.org/10.1061/(asce)st.1943-541x.0002544.

[12] A. Elkady, D.G. Lignos, Dynamic stability of deep and slender wide-flange steel columns - Full scale experiments, in: Struct. Stab. Res. Counc. Annu. Stab. Conf. 2016, SSRC 2016, 2016.

[13] C.A. Trautner, T. Hutchinson, P.R. Grosser, J.F. Silva, Investigation of steel column–baseplate connection details incorporating ductile anchors, J. Struct. Eng. (2017), https://doi.org/10.1061/(asce)st.1943-541x.0001759.

[14] J.G. Soules, R.E. Bachman, J.F. Silva, Chile Earthquake of 2010: Assessment of Industrial Facilities around Concepción, American Society of Civil Engineers, 2016, https://doi.org/10.1061/9780784413647.

[15] A.S. Hassan, B. Song, C. Galasso, A. Kanvinde, Seismic performance of exposed column–base plate connections with ductile anchor rods, J. Struct. Eng. 148 (2022) 1–19, https://doi.org/10.1061/(asce)st.1943-541x.0003298.

[16] C. Trautner, T. Hutchinson, M. Copellini, P. Grosser, R. Bachman, J. Silva, Developing ductility using concrete anchorage, ACI Struct. J. (2017), https://doi.org/10.14359/51689152.

[17] J.E. Parks, C.P. Pantelides, L. Ibarra, D.H. Sanders, Stretch length anchor bolts under combined tension and shear, ACI Struct. J. (2019), https://doi.org/10.14359/51702236.

[18] F. Zareian, A. Kanvinde, Effect of column-base flexibility on the seismic response and safety of steel moment-resisting frames, Earthquake Spectra (2013), https://doi.org/10.1193/030512EQS062M.

[19] A. Zingoni, Shell Structures in Civil and Mechanical Engineering, 2nd edition, ICE Publishing, 2017, https://doi.org/10.1680/ssicame.60289.437.

[20] M.A. Shaheen, M.A. Galal, L.S. Cunningham, A.S.J. Foster, New technique to improve the ductility of steel beam to column bolted connections: a numerical investigation, CivilEng 2 (2021) 929–942.

[21] M.A. Shaheen, A.S.J. Foster, L.S. Cunningham, A novel device to improve robustness of end plate beam–column connections: analytical model development, Thin-Walled Struct. 172 (2022), 108878, https://doi.org/10.1016/j.tws.2021.108878.

[22] M.A. Shaheen, A new idea to improve the cyclic performance of end plate beam–column connections, Eng. Struct. 253 (2022), 113759, https://doi.org/10.1016/j.engstruct.2021.113759.

[23] M.A. Shaheen, A.S. Andrew, L.S. Cunningham, A novel device to improve robustness of end plate beam-column connections, Structures 28 (2020) 2415–2423.

[24] A. Picard, D. Beaulieu, Behaviour of a simple column base connection, Can. J. Civ. Eng. (1985), https://doi.org/10.1139/l85-013.

[25] ABAQUS, Abaqus 6.19, Dassault Systèmes Simulia Corp, Provid RI, USA, 2019.

[26] C.A. Trautner, T.C. Hutchinson, Parametric finite-element modeling for exposed steel moment frame column baseplate connections subjected to lateral loads, J. Struct. Eng. (2018) 144, https://doi.org/10.1061/(asce)st.1943-541x.0001990.

[27] A.S. Hassan, P. Torres-Rodas, L. Giulietti, A. Kanvinde, Strength characterization of exposed column base plates subjected to axial force and biaxial bending, Eng. Struct. (2021) 237, https://doi.org/10.1016/j.engstruct.2021.112165.

[28] S. Jordan Jr., Finite Element Simulations of Exposed Column Base Plate Connections Subjected to Axial Compression and Flexure, UNIVERSITY OF CALIFORNIA DAVIS, 2010.

[29] I.R. Gomez, Behavior and Design of Column Base Connections, University of California, Davis, 2010.

[30] P. Torres-Rodas, M. Medalla, F. Zareian, D. Lopez-Garcia, Cyclic behavior and design methodology of exposed base plates with extended anchor bolts, Eng. Struct. 260 (2022), 114235, https://doi.org/10.1016/j.engstruct.2022.114235.

[31] BS EN 1992-1-1, Eurocode 2: Design of Concrete Structures - Part 1–1: General Rules And rules for Buildings, Br Stand Inst, 2004.

[32] F. Delhomme, G. Debicki, Z. Chaib, Experimental behaviour of anchor bolts under pullout and relaxation tests, Constr. Build. Mater. (2010), https://doi.org/10.1016/j.conbuildmat.2009.08.038.

[33] CEN, BS EN 1993-1-2:1995 - Eurocode 3: Design of Steel Structures - Part 1–2: General Rules - Structural Fire Design. Eurocode 3, 1995.

[34] ASCE, ASCE/SEI 41–17: American Society of Civil Engineers: Seismic Evaluation and Retrofit of Existing Buildings, American Society of Civil Engineers, 2017.

[35] K.Y. Dai, X.H. Yu, D.G. Lu, Phenomenological hysteretic model for corroded RC columns, Eng. Struct. (2020), https://doi.org/10.1016/j.engstruct.2020.110315.

[36] C.B. Haselton, A.B. Liel, S.C. Taylor-Lange, G.G. Deierlein, Calibration of model to simulate response of reinforced concrete beam-columns to collapse, ACI Struct. J. (2016), https://doi.org/10.14359/51689245.

[37] E.L. Grimsmo, A.H. Clausen, M. Langseth, A. Aalberg, An experimental study of static and dynamic behaviour of bolted end-plate joints of steel, Int. J. Impact. Eng. 85 (2015) 132–145, https://doi.org/10.1016/j.ijimpeng.2015.07.001.